Electronic Supplementary Material (ESI) for Nanoscale

Supporting Informations

Nanomagnetism reveals the intracellular clustering of iron oxide nanoparticles in the organism

Michael Levy[1], Claire Wilhelm[1], Nathalie Luciani[1], Vanessa Deveaux[2], François Gendron[3], Alain Luciani[2], Martin Devaud[1] and Florence Gazeau[1*]

Theoretical appendix

Superparamagnetic behaviour of nanomagnets: effect of local distribution and magnetic interactions.

Superparamagnetic behaviour of single-domain ferrite nanocrystals is characterized by thermal fluctuations of their magnetic moment with respect to the crystal lattice. The magnetic moment can spontaneously flip from one easy axis to another with a characteristic time called the Néel relaxation time. In the absence of any external field, the Néel time τ_N increases exponentially with the ratio of the anisotropy energy barrier (usually proportional to the particle volume) to the thermal energy kT. In an external magnetic field, a direction of the magnetic moment is preferred and the energy landscape is no longer symmetric. The Néel time is thus modified according to the total local magnetic field experienced by the particle.

The magnetization $M(B)$ of an assembly of superparamagnetic nanoparticles as a function of the applied magnetic field B fits a Langevin law $\mu L(\xi)$ (where $\xi = \mu B / kT$ is the Langevin parameter and $\mu = \pi M_s d^3 / 6kT$ the magnetic moment of each particle) weighted by a log-normal distribution of particle diameter d: $P(d) = 1/(\sqrt{2\pi}\sigma d) \times \exp(-\ln^2(d/d_0)/2\sigma^2)$ where σ is the polydispersity index, d_0 the characteristic diameter. It is thus possible to deduce the NP size distribution from the fit of the magnetization curve at 300K, when all NPs are superparamagnetic.

A classical method to probe the Néel dynamics of an assembly of polydisperse nanoparticles is to measure its global static magnetization as a function of temperature. At a temperature close to 0K, the magnetization of a zero-field cooled (ZFC) sample is null, because the magnetic moments are blocked in random directions (τ_N is larger than the time of the measurement t_{exp}). With increasing temperature, thermal fluctuations allow the magnetic moment of the smallest particles to overcome the energy barrier during the time of the measurement ($\tau_N < t_{exp}$) and to partially align along the applied field. Accordingly, the global magnetization M increases with the number of nanoparticles that have transited in the superparamagnetic state. The ZFC magnetization reaches a maximum at the so-called "blocking temperature" T_B, when most of magnetic moments are no longer blocked. Beyond

T_B, the magnetization turns to decrease with temperature due to the thermal averaging of the direction of magnetic moments.

For non-interacting NPs (e.g. in dilute colloidal suspension), the temperature dependence of the ZFC magnetization (measured at 50 Gauss) is characteristic of the nanoparticle size distribution (determined from $M(B)$ at 300K) and can be fitted accordingly following a classical theory. At a given temperature in an applied magnetic field B_0, the nanoparticles in the blocked state (*b*) are distinguished from nanoparticles in the superparamagnetic state (*sp*) depending on their Néel time $\tau_N(d,T,B_0)$ compared to the time of the measurement. Only the (*sp*) nanoparticles contribute to the global magnetization, each of them following a Langevin function $\langle\mu\rangle(d,T,B_0)=\mu L(\xi_0)$.

We extended the classical theory to take magnetic interactions between nanoparticles within intracellular compartments into account. Interacting NPs experience a local field, which no more reduces to the external magnetic field $\vec{B}_0$, but also accounts for the dipolar fields created by all the surrounding nanoparticles. As a consequence, the Néel time $\tau_N(d,T,\vec{B}_{loc})$, as well as the mean magnetic moment along $\vec{B}_0 = B_0\vec{u}_z$, also depend on the local magnetic field $\vec{B}_{loc} = B_{loc}\vec{u}_{loc}$ experienced by the NP: $\langle\mu_z\rangle(d,T,\vec{B}_{loc})=\mu L(\xi_{loc})\vec{u}_{loc}.\vec{u}_z$. The calculation of the local field is detailed elsewhere[1]. We simply give here the deciding factors that influence the superparamagnetic behaviour of interacting NPs. Typically the dipolar field created at a distance of 8 nm, around a typical maghemite nanoparticle is of the order of 300 Gauss and thus by far exceeds the applied external field (50 Gauss). The dipolar field decreases as $1/l^3$, where l is the distance from the source NP. We assume a spherical geometry for the intracellular structures containing NPs. For symmetry reasons, the interaction effect resulting from all NPs on a given nanoparticle reduces to the very local influence of the neighbours in closest proximity, because the contributions of all other nanoparticles tend to vectorially compensate each other. We thus define r as the mean local volume fraction of neighbours. The global magnetization $M_z(T)$ can be calculated numerically by summing $\langle\mu_z\rangle(d,T,\vec{B}_{loc})$ over the size distribution of (*sp*) nanoparticles (with the Néel $\tau_N(d,T,\vec{B}_{loc})$ now depending on $\vec{B}_{loc}$) and over the probability density of vectorial $\vec{B}_{loc}$. When the local volume fraction *r* of neighbours increases, this model predicts an increase of the blocking temperature T_B and a decrease of the magnetization at T_B (Figure 4A), as observed experimentally for cell-internalized NPs. Interestingly, we can estimate the

mean local field experienced by interacting NPs: it is always larger than B_0, it increases with r and tends to B_0 when the temperature rises. This enhancement of the local field strongly affects the dynamical behaviour of the NPs assembly. The Néel time for a given particle size is reduced and distributed due to the variability of direction and intensity of $\vec{B}_{loc}$. The blocked-to-superparamagnetic transition for a given size occurs at slightly lower temperatures in presence of interactions. The magnetization is diminished due to the orientational distribution of local fields, which impede the alignment of magnetic moments along the external field B_0. Each nanoparticle is influenced by the dynamics of its neighbours being in the (*sp*) or (*b*) state. The blocking temperature T_B, defined as the temperature of the maximum ZFC magnetization, no longer reflects the temperature of the (*b*)-to-(*sp*) transition, but is shifted towards higher temperatures by interaction effects, which decrease with temperature. The influence of the (*sp*) NPs onto the local field tends indeed to diminish with increasing temperature. Note that this model is only valid for local fields lower than the anisotropy field (of the order of 1100 Gauss for maghemite nanoparticles), which imposes an upper limit for r (typically r =0.3). We also considered that intracellular structures containing NPs were sufficiently diluted in the cell to neglect any interaction between them. To sum up, we have shown that interactions effects due to the local distribution of nanoparticles in intracellular structures are quantitatively evidenced by the temperature dependence of static ZFC magnetization measurements.

1. M. Levy, F. Gazeau, J. C. Bacri, C. Wilhelm and M. Devaud, *Phys Rev B*, 2011, **84**, 075480-075491

2. M. Levy, N. Luciani, D. Alloyeau, D. Elgrabli, V. Deveaux, C. Pechoux, S. Chat, G. Wang, N. Vats, F. Gendron, C. Factor, S. Lotersztajn, A. Luciani, C. Wilhelm and F. Gazeau, *Biomaterials*, 2011, **32**, 3988-3999.

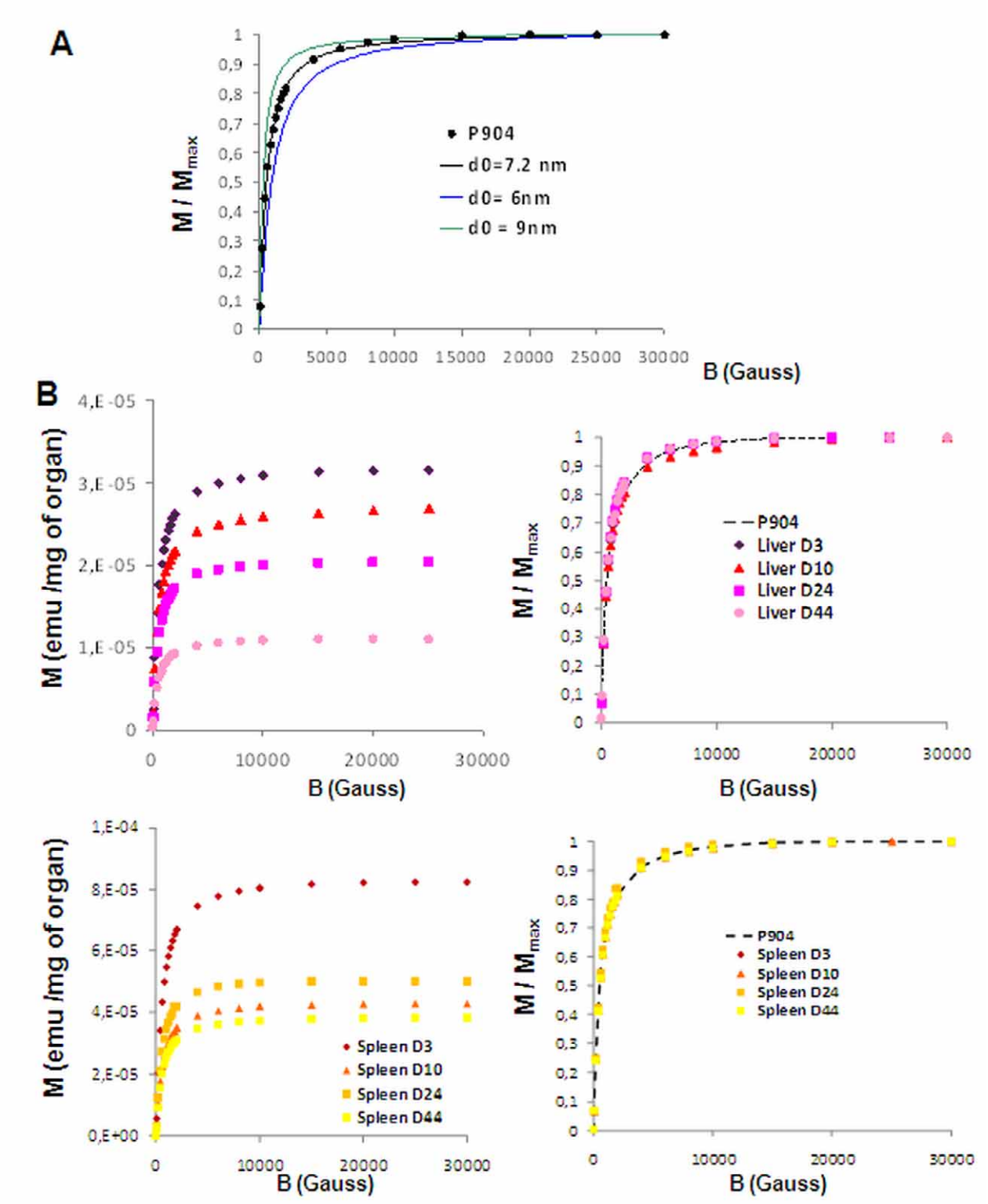

Figure SI-1 : A- Normalized magnetization as a function of magnetic field strength measured at 300K for P904 nanoparticles in colloidal suspension (black point). Theoretical magnetization curves are displayed, corresponding to the size distribution of P904 NPs ($d_0 = 7.2$ nm, σ=0.24 (black line)) and to slightly lower or higher diameters ($d_0 = 6$ nm (blue line) and $d_0 = 8.2$ nm (green line), σ=0.24). It illustrates the sensitivity of magnetization curves to any change in the NP size. B- Magnetization curves for liver (top) and spleen (bottom) samples at days 3, 10, 24 and 44 following high dose administration of P904. For comparison the magnetization curves of P904 colloidal suspension is displayed in shaded line. Liver and spleen magnetization per mg of fresh organ diminish with time. Once normalized by the saturation magnetization, the field dependence of liver and spleen magnetization are identical to that of P904 and remain unchanged with time after administration (right). This finding reveals the stability of NPs size distribution in the organs up to 44 days after high dose injection.

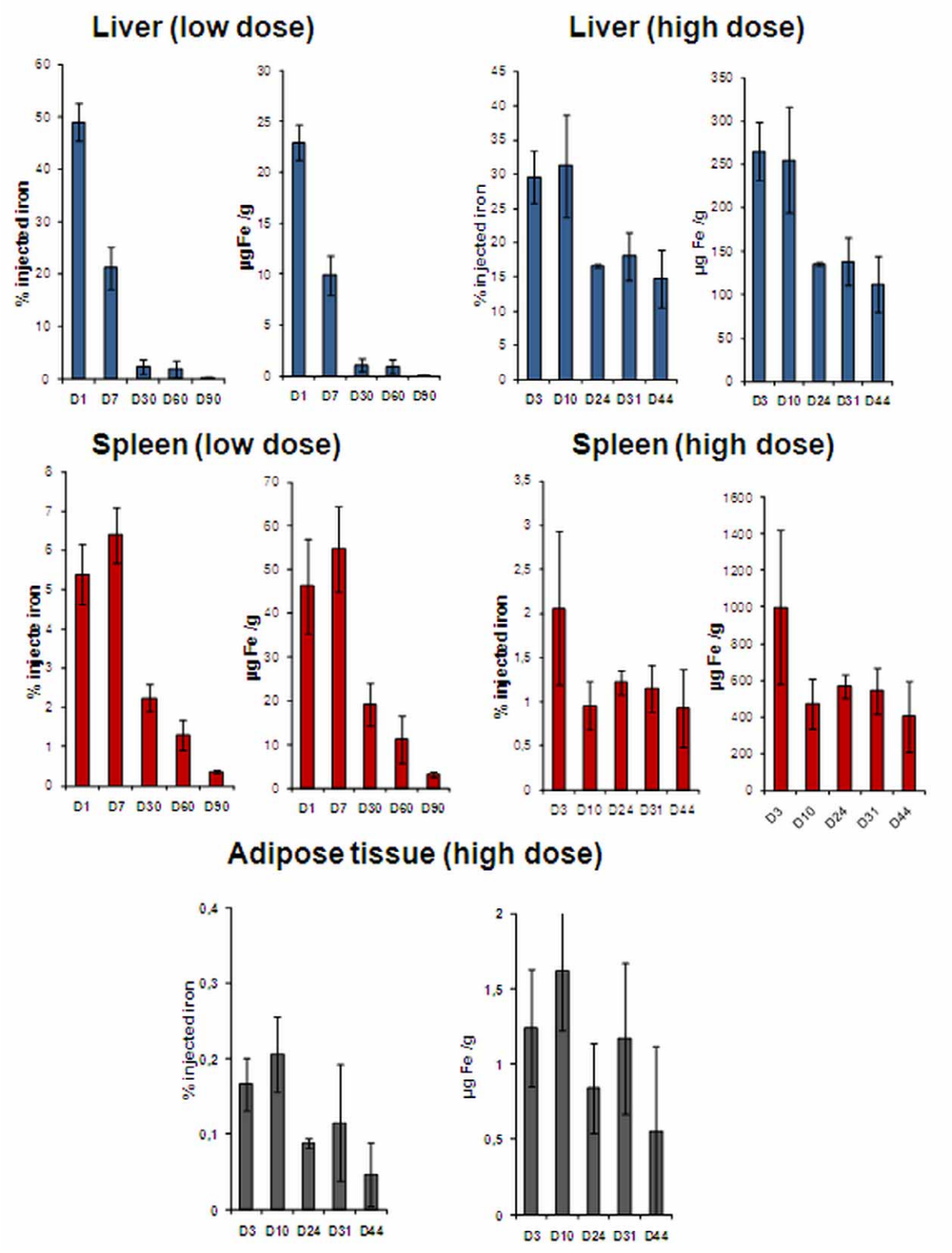

Figure SI-2 : Quantification of P904 nanoparticles content in organs as a function of time after injection (in days). The P904 concentration was determined by Ferromagnetic Resonance (FMR) experiment performed on dried organs as described in details in Levy et al

[2]. This method allows to specifically quantify the superparamagnetic nanoparticles in a biological sample, making free of contributions coming from endogenous non-magnetic forms of iron. The P904 content is here expressed as a percentage of the total iron mass which has been injected (62 µg for the low dose and 2630 µg for the high dose). In addition, we also displayed the P904 concentration in the organ expressed as microgram of iron per gram of fresh organ. The degradation/biotransformation of P904 nanoparticles is almost completed by three months after low dose injection. In contrast, after high dose injection, the degradation process is not completed after 44 days. Note that the P904 content in adipose tissue represents less than 0.2% of the injected dose.